

Forward-backward angle asymmetry and polarization observables in high-energy deuteron photodisintegration

V.Yu. Grishina ^a, L.A. Kondratyuk ^b, W. Cassing ^c, E. De Sanctis ^d, M. Mirazita ^d, F. Ronchetti ^d and P. Rossi ^d

^a Institute for Nuclear Research, 60th October Anniversary Prospect 7A, 117312 Moscow, Russia

^b Institute for Theoretical and Experimental Physics, B. Cheremushkinskaya 25, 117218 Moscow, Russia

^c Institute for Theoretical Physics, University of Giessen, Heinrich-Buff-Ring 16, D-35392 Giessen, Germany

^d INFN-Laboratori Nazionali di Frascati, CP 13, via E. Fermi, 40; I-00044, Frascati, Italy

Received: date / Revised version: date

Abstract. Deuteron two-body photodisintegration is analysed within the framework of the Quark-Gluon Strings Model. It is found that the forward-backward angle asymmetry predicted by the model is confirmed by the recent data at different photon energies from Jlab. New calculations for polarization observables, the cross section asymmetry Σ and the polarization transfer $C_{2'}$, for photon energies (1.2 ÷ 6) GeV are presented and compared with the data available up to 2 GeV.

PACS. 13.40.-f Electromagnetic processes and properties – 25.20.-x Photonuclear reactions

1 Introduction

Experiments on high energy two-body photodisintegration of the deuteron [1,2] have shown that the cross section data at proton angles $\theta_p^{\text{CM}} = 89^\circ$ and 69° exhibit scaling consistent with the constituent quark counting rule behavior [3]¹ for photon energies $E_\gamma \geq 1$ GeV while at forward angles, $\theta_p^{\text{CM}} = 36^\circ$ and 52° , scaling is not observed for $E_\gamma \leq 4$ GeV. Moreover, the data on the recoil polarization for the $d(\vec{\gamma}, \vec{p})n$ reaction at $\theta_p^{\text{CM}} = 90^\circ$ for photon energies up to 2.4 GeV [4] do not support the helicity conservation as predicted by perturbative QCD (pQCD). Thus scaling is no longer considered as sufficient evidence for the applicability of pQCD in the energy range $E_\gamma = (1 \div 4)$ GeV and nonperturbative approaches should be applied, too.

To this aim, recently, some of us have studied the high-energy deuteron photodisintegration within the framework of the Quark-Gluon Strings Model (QGSM) [5,6]. This model - proposed by Kaidalov [7,8] - is based on two ingredients: i) a topological expansion in QCD and ii) a space-time picture of the interactions between hadrons that takes into account the confinement of quarks. In a more general sense the QGSM can be considered as a microscopic (nonperturbative) model of Regge phenomenology for the analysis of exclusive and inclusive hadron-hadron and photon-hadron reactions on the quark level.

We recall that originally the QGSM has been formulated for small scattering angles or low 4-momentum transfer (squared) t

(here t , u and s are the usual Mandelstam variables). The question thus arises, how to extrapolate the QGSM amplitudes to large angles (or large t). Following Coon et al. [9] we assume that there is only a single analytic Regge term that smoothly connects the small angle and fixed-large-angle regions. Thus, according to Ref.[10], we require that the amplitude at fixed angle should be obtained either as the large t limit of the forward Regge form or as the large u limit of the backward Regge form. The only solution to these boundary conditions is a logarithmic decreasing trajectory,

$$\alpha_N(t) = \alpha_N(-T_B) - d \ln(-t/T_B), \quad (1)$$

where d is a constant and T_B is a scale parameter. Such a form of the Regge trajectory naturally arises in the logarithmic dual model (LDM), that very well describes the differential cross section $d\sigma/dt$ for elastic pp scattering in the energy range (5 ÷ 24) GeV for $-t$ up to 18 GeV² [9]. It is worth noticing that logarithmic form of non-linear Regge trajectories have also been discussed in Refs. [11, 12, 13, 14]. The special case with $d = 0$ corresponds to 'saturated' trajectories, which means that all the trajectories approach a constant at large negative t . We recall, that this case leads to the constituent-interchange model which is a predecessor of the asymptotic quark-counting rules [3, 15]. The approach with 'saturated' trajectories was successfully used to explain the large t behavior of hadron and photon induced reactions in Refs. [16, 17, 18, 19].

Within the QGSM the deuteron photodisintegration amplitude $T(\gamma d \rightarrow pn)$ can be described in first approximation by planar graphs with three valence quark exchange in t (or u)-channels, which corresponds to a nucleon Regge trajectory (see Fig. 1). In Ref. [5] deuteron photodisintegration has been ana-

¹ i.e. at fixed c.m. angle the differential cross section $d\sigma/dt_{\gamma d \rightarrow pn}$ scales as $\sim s^{-11}$

lyzed using nonlinear Regge trajectories. It was found that the QGSM provides a reasonable description of the Jlab data on deuteron photodisintegration at large momentum transfer t [1] when using a logarithmic form for the nucleon trajectory similar to that of Eq. (1). This has provided new evidence for a nonlinearity of the Regge trajectory $\alpha_N(t)$.

In this work we compare the predictions of the QGSM with all data available at high energies [1, 2, 20, 21, 22, 23, 24, 25, 26, 27] and provide a more detailed analysis of the forward-backward angle asymmetry. Moreover, as a novel aspect we calculate the cross section asymmetry Σ and the polarization transfer to the proton C_z in the reaction $\vec{\gamma}d \rightarrow \vec{p}n$ for photon energies $E_\gamma = (1.2 \div 6)$ GeV and compare them to the data available at $\theta_p^{\text{CM}} = 90^\circ$ and up to 2 GeV [4, 28].

The layout of the paper is as follows: In Section 2 the spin structure of the $\gamma d \rightarrow pn$ amplitude is evaluated and in Section 3 the analysis of the forward-backward asymmetry is discussed. In Section 4 the results (and predictions) of the QGSM are compared with the available data for the energy dependence of the differential cross section at fixed angles. Section 5 is devoted to the definition and calculation of polarization observables while Section 6 summarises the results of the work.

2 Spin structure of the $\gamma d \rightarrow pn$ amplitude

As already mentioned above the main assumption of the QGSM is that the deuteron photodisintegration amplitude $T(\gamma d \rightarrow pn)$ can be described by planar graphs with three valence quark exchange in t - or u - channels with any number of gluon exchanges between them (cf. Fig.1). This corresponds to the contributions of the t - and u - channel nucleon Regge trajectories. In the space-time picture the intermediate s -channel consists of a $6q$ string (or color tube) with q and $5q$ states at the ends.

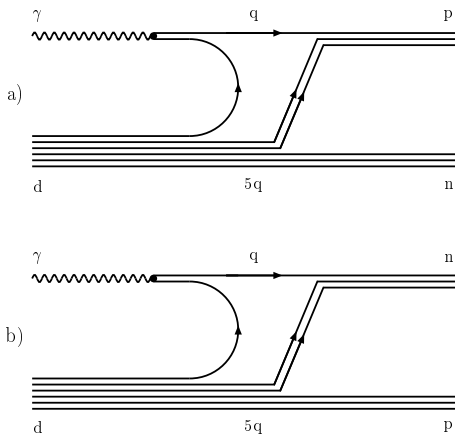


Fig. 1. Diagrams for deuteron photodisintegration describing three valence quark exchanges in the t - (a) and u -channel (b).

The spin dependence of the $\gamma p \rightarrow pn$ amplitude has been evaluated in Ref. [5] in a simple way by assuming that all intermediate quark clusters have minimal spins and the s -channel helicities in the quark-hadron and hadron-quark transition amplitudes are conserved. In this limit the spin structure of the

amplitude $T(\gamma d \rightarrow pn)$ can be written as (see Ref. [5], comment after Eq. (27))

$$\langle p_3, \lambda_p; p_4, \lambda_n | \hat{T}(s, t) | p_2, \lambda_d; p_1, \lambda_\gamma \rangle \simeq \bar{u}_{\lambda_p}(p_3) \hat{\epsilon}_{\lambda_\gamma} [A(s, t)(\hat{p}_3 - \hat{p}_1) + B(s, t)m] \hat{\epsilon}_{\lambda_d} v_{\lambda_n}(p_4), \quad (2)$$

where m is the nucleon mass, p_1, p_2, p_3 , and p_4 are the 4-momenta of the photon, deuteron, proton, and neutron, respectively, and λ_i denotes the s channel helicity of the i -th particle. The invariant amplitudes $A(s, t)$ and $B(s, t)$ have similar Regge asymptotics (see below). It is possible to show (cf. Ref. [5]) that at small scattering angles the ratio $R = A(s, t)/B(s, t)$ is a smooth function of t and can be considered as an effective constant that depends on the ratio of the nucleon mass to the constituent quark mass m_q : $R \simeq m/(2m_q)$. It is interesting to note that the spin structure of the $\gamma d \rightarrow pn$ amplitude in Eq. (2) is very similar to the amplitude within the Reggeized Nucleon Born Term Model (see Refs. [16, 29]) where the ratio $R = A/B = 1$ is directly related to the nucleon propagator. In line with Ref. [5] we also treat the ratio R as a constant value that, however, may range between 1 and 2.5.

The differential cross section for the reaction $\gamma d \rightarrow pn$ is

$$\frac{d\sigma_{\gamma d \rightarrow pn}}{dt} = \frac{1}{64\pi s} \frac{1}{(p_{\gamma \text{cm}})^2} \times \left[S_t \left| B^{(+)}(s, t) \right|^2 + S_u \left| B^{(-)}(s, u) \right|^2 + 2S_{tu} \text{Re} \left(B^{(+)}(s, t) B^{(-)*}(s, u) \right) \right], \quad (3)$$

where the amplitudes $B^{(\pm)}(s, t) = B^{(\rho)}(s, t) \pm B^{(\omega)}(s, t)$ are combinations of the contributions from isovector (ρ like) and isoscalar (ω like) photons. The kinematical functions S_t, S_u, S_{tu} in (3) can be written in a covariant form as

$$\begin{aligned} S_t &= \frac{1}{6} \sum_{\lambda_\gamma, \lambda_d} \text{Sp} \left[\hat{\epsilon}_{\lambda_\gamma} (R(\hat{p}_3 - \hat{p}_1) + m) \hat{\epsilon}_{\lambda_d} (\hat{p}_4 - m) \right. \\ &\quad \left. \times \hat{\epsilon}_{\lambda_d}^* (R(\hat{p}_3 - \hat{p}_1) + m) \hat{\epsilon}_{\lambda_\gamma}^* (\hat{p}_3 + m) \right], \\ S_u &= \frac{1}{6} \sum_{\lambda_\gamma, \lambda_d} \text{Sp} \left[\hat{\epsilon}_{\lambda_d} (R(\hat{p}_4 - \hat{p}_1) - m) \hat{\epsilon}_{\lambda_\gamma} (\hat{p}_4 - m) \right. \\ &\quad \left. \times \hat{\epsilon}_{\lambda_\gamma}^* (R(\hat{p}_4 - \hat{p}_1) - m) \hat{\epsilon}_{\lambda_d}^* (\hat{p}_3 + m) \right], \\ S_{tu} &= -\frac{1}{6} \sum_{\lambda_\gamma, \lambda_d} \text{Sp} \left[\hat{\epsilon}_{\lambda_\gamma} (R(\hat{p}_3 - \hat{p}_1) + m) \hat{\epsilon}_{\lambda_d} (\hat{p}_4 - m) \right. \\ &\quad \left. \times \hat{\epsilon}_{\lambda_\gamma}^* (R(\hat{p}_4 - \hat{p}_1) - m) \hat{\epsilon}_{\lambda_d}^* (\hat{p}_3 + m) \right] \quad (4) \end{aligned}$$

In order to achieve consistency of the differential cross section $d\sigma/dt$ with Regge asymptotics for large s and fixed t , we use the following parametrization of the amplitude $B^{(+)}(s, t)$

$$\left| B^{(+)}(s, t) \right|^2 = \frac{1}{C_0 p_{\gamma \text{cm}}^2} |\mathcal{M}_{\text{Regge}}(s, t)|^2, \quad (5)$$

where $C_0 = (36 \pm 3) \text{ GeV}^2$ and

$$\mathcal{M}_{\text{Regge}}(s, t) = F(t) \left(\frac{s}{s_0} \right)^{\alpha_N(t)} \exp \left[-i \frac{\pi}{2} \left(\alpha_N(t) - \frac{1}{2} \right) \right]. \quad (6)$$

Here $\alpha_N(t)$ is the trajectory of the nucleon Regge pole and $s_0 = 4 \text{ GeV}^2 \simeq m_d^2$ (m_d denoting the mass of the deuteron). We take the dependence of the residue $F(t)$ on t in the form

$$F(t) = B_{\text{res}} \left[\frac{1}{m^2 - t} \exp(R_1^2 t) + C \exp(R_2^2 t) \right] \quad (7)$$

as it has been used in Refs. [30,31] for the description of the reactions $pp \rightarrow d\pi^+$ and $\bar{p}d \rightarrow p\pi^-$ at $-t \leq 1.6 \text{ GeV}^2$. In Eq. (7) the first term in the square brackets contains the nucleon pole and the second term ($\sim C$) accounts for the contribution of non-nucleonic degrees of freedom in the deuteron.

The amplitude defined by Eq. (3) has a rather simple covariant structure and can be extrapolated to large angles. As shown in Ref. [5] the energy behavior of the cross section crucially depends on the form of the Regge trajectory $\alpha_N(t)$ for large negative t . The form, that better describes the data, is the logarithmic one with nonleading contributions:

$$\alpha_N(t) = \alpha_N(0) - \alpha'_N(0) T_B \ln(1 - t/T_B). \quad (8)$$

Here we use this trajectory with $\alpha_N(0) = -0.5$, $\alpha'_N(0) = 0.9 \text{ GeV}^{-2}$, and $T_B = 1.7 \text{ GeV}^2$; furthermore, we take $R = A(s, t)/B(s, t) = 2$ and adopt the following values for the parameters of the residue $F(t)$ in Eq. (7):

$$B_{\text{res}} = 2.05 \cdot 10^{-4} \text{ kb}^{1/2} \text{ GeV}, \quad C = 0.7 \text{ GeV}^{-2}, \\ R_1^2 = 2 \text{ GeV}^{-2}, \quad R_2^2 = 0.03 \text{ GeV}^{-2}. \quad (9)$$

Note that these parameters, except for the overall normalization factor B_{res} , are not very different from those determined by fitting data on the reaction $pp \rightarrow \pi^+ d$ at $-t \leq 1.6 \text{ GeV}^2$ [30]. In our case, C remains unchanged and the factor B_{res} and the radii R_1^2 and R_2^2 have been fixed using two experimental values of the deuteron photodisintegration cross section at 1.6 GeV and $\theta_p^{\text{CM}} = 36^\circ$ and 52° . These parameters are the same as in Ref. [5], apart from a small (about 13%) readjustment of B_{res} ($2.05 \cdot 10^{-4} \text{ kb}^{1/2} \text{ GeV}$, instead of $1.8 \cdot 10^{-4} \text{ kb}^{1/2} \text{ GeV}$). This is due to the fact that in the present work the energy dependence of the differential cross section has been calculated taking into account two amplitudes that describe the contribution of isovector (ρ like) and isoscalar (ω like) photons (see Eq. (3)), while in Ref. [5] the isovector photon dominance (i.e. $B^\omega = 0$) was assumed.

Adopting the Vector Meson Dominance (VMD) model we get

$$B^\omega(s, t) = B^\rho(s, t)/\sqrt{8}, \quad B^\omega(s, u) = B^\rho(s, u)/\sqrt{8}. \quad (10)$$

3 Angular distributions and forward-backward angle asymmetry

As argued in Ref. [5] a forward-backward angle asymmetry in the angular distribution in the reaction $\gamma d \rightarrow pn$ arises from the interference of the isovector and isoscalar amplitudes. In Fig. 2 we present the angular dependence of $d\sigma/d\Omega$ (dashed lines) at four photon energies $E_\gamma = 1.1 \text{ GeV}$, 1.6 GeV , 1.9 GeV , and 2.4 GeV . The QGSM calculations are found to be in very

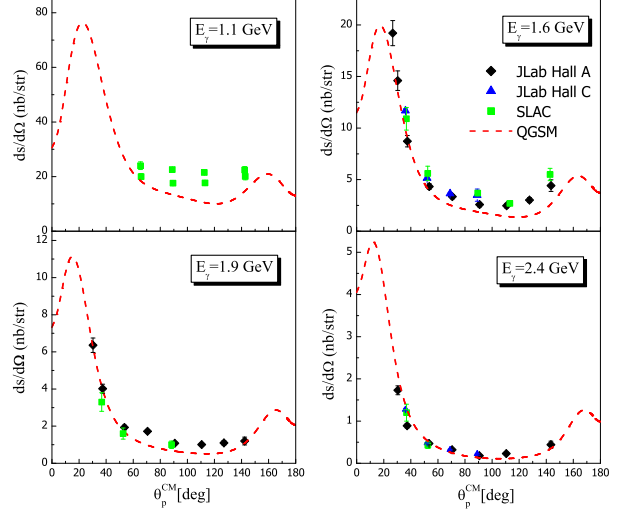


Fig. 2. The differential cross section for the reaction $\gamma d \rightarrow pn$ as a function of the proton angle θ_p^{CM} for different photon energies E_γ from the QGSM (dashed lines). The experimental data are from SLAC [21, 22, 23], Jlab-Hall C [1] and Jlab-Hall A [24].

good agreement with the experimental data taken from Refs. [1, 21, 22, 23, 24] and also with the new preliminary data from Jlab-Hall B, (not shown in the figure), which determine almost the full angular distributions [25, 26, 27]. These latter data, in particular, clearly support the predicted forward-backward angle asymmetry (see Fig. 3 of Ref. [25] and Fig. 2 of Ref. [26]). The calculated angular distributions have a dip for $\theta_p^{\text{CM}} = 0^\circ$ and 180° which is related to the choice of the ratio $R = A(s, t)/B(s, t) = 2$. This dip does not appear for $R = 1$, which corresponds to the limit of the Reggeized Nucleon Born Term Model (cf. Section 2). As argued in Ref. [25] a full analysis of the data from Jlab-Hall B will allow to prove/disprove the appearance of the dips predicted by the QGSM.

4 Energy dependence of the differential cross section

The QGSM predicts, furthermore, that the differential cross section $d\sigma/dt$ at fixed θ_p^{CM} angles decreases faster than any finite power of s and that at sufficiently large energies the perturbative regime will become dominant. Moreover, as it was shown in Ref. [5], the model well describes the energy dependence of $d\sigma/dt \cdot s^{11}$ at different θ_p^{CM} angles for photon energies of $(1 \div 4) \text{ GeV}$. This is shown in Fig. 3 where the QGSM predictions for the energy dependence of $d\sigma/dt \cdot s^{11}$ at four θ_p^{CM} angles - calculated for the logarithmic nonlinear trajectory (dashed lines) - are compared with all data available at high energies: Mainz [20], SLAC [21, 22, 23], Jlab-Hall A [24] and Jlab-Hall C [1, 2]. One can see that above 4 GeV the QGSM overestimates the data at $\theta_p^{\text{CM}} = 36^\circ$ and systematically underpredicts the data at $\theta_p^{\text{CM}} = 89^\circ$. These discrepancies might be

attributed to the simplifying assumption that all the intermediate quark clusters have minimal spins. Moreover, the ratio $R = A/B$ may also deviate from a constant at large momentum transfer t . For a better understanding of the situation new data at intermediate angles appear to be important.

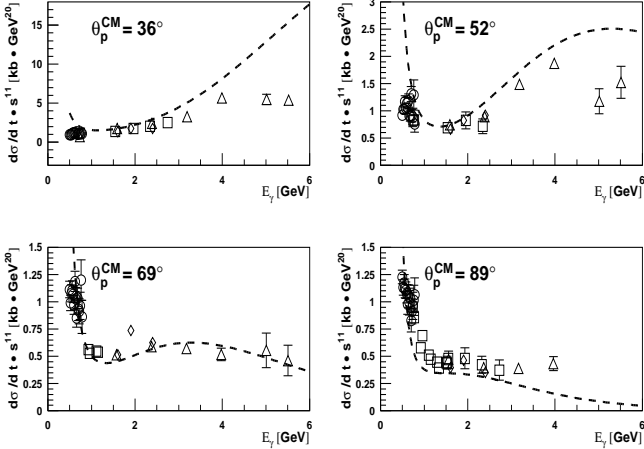


Fig. 3. The differential cross section for the reaction $\gamma d \rightarrow pn$ (multiplied by s^{11}) as a function of the photon lab. energy E_γ at different proton angles θ_p^{CM} in the center-of-mass frame in comparison to the experimental data from Mainz [20], SLAC [21,22,23], Jlab-Hall C [1,2] and Jlab-Hall A [24]. The dashed lines are calculated within the QGSM using the logarithmic nucleon Regge trajectory (8).

5 Polarization observables

The energy dependence of the photodisintegration cross section has been shown to be a potentially misleading indicator for the success of pQCD. Models with asymptotic behaviour, which differ from pQCD, fit the data as well or even better than pQCD (see e.g. Refs. [5, 15, 32, 33, 34]). Thus further theoretical developments and experimental tests of nonperturbative quark models will be necessary. To this aim, polarization observables are very important to further constrain the different approaches.

For the definitions of these observables in terms of helicity amplitudes we refer the reader to Ref. [35]. We briefly recall here the necessary notations and definitions:

$$F_{i,\pm} = \langle \lambda_p; \lambda_n | \hat{T}(s, t) | \lambda_\gamma; \lambda_d \rangle, \quad (11)$$

where

$$F_{1,\pm} = \langle \pm \frac{1}{2}; \pm \frac{1}{2} | \hat{T}(s, t) | 1; 1 \rangle, \quad (12)$$

$$F_{2,\pm} = \langle \pm \frac{1}{2}; \pm \frac{1}{2} | \hat{T}(s, t) | 1; 0 \rangle, \quad (13)$$

$$F_{3,\pm} = \langle \pm \frac{1}{2}; \pm \frac{1}{2} | \hat{T}(s, t) | 1; -1 \rangle, \quad (14)$$

$$F_{4,\pm} = \langle \pm \frac{1}{2}; \mp \frac{1}{2} | \hat{T}(s, t) | 1; 1 \rangle, \quad (15)$$

$$F_{5,\pm} = \langle \pm \frac{1}{2}; \mp \frac{1}{2} | \hat{T}(s, t) | 1; 0 \rangle, \quad (16)$$

$$F_{6,\pm} = \langle \pm \frac{1}{2}; \mp \frac{1}{2} | \hat{T}(s, t) | 1; -1 \rangle. \quad (17)$$

The angular distribution in terms of the helicity amplitudes then is given by

$$f(\theta) = \sum_{i=1}^6 \sum_{\pm} |F_{i,\pm}|^2, \quad (18)$$

while the polarization observables, i.e. the induced polarization, P_y , the cross section asymmetry, Σ , and the polarization transfers, $C_{x'}$, $C_{z'}$ are defined via:

$$f(\theta) P_y = 2 \text{Im} \sum_{i=1}^3 [F_{i,+}^* F_{i+3,-} - F_{i,-}^* F_{i+3,+}], \quad (19)$$

$$f(\theta) \Sigma = -2 \text{Re} \left[\sum_{\pm} (F_{1,\pm}^* F_{3,\mp} - F_{4,\pm} F_{6,\mp}^*) - F_{2,+}^* F_{2,-} + F_{5,+}^* F_{5,-} \right], \quad (20)$$

$$f(\theta) C_{x'} = 2 \text{Re} \sum_{\pm} [F_{1,\pm} F_{4,\mp}^* + F_{2,\pm} F_{5,\mp}^* + F_{3,\pm} F_{6,\mp}^*], \quad (21)$$

$$f(\theta) C_{z'} = \sum_{i=1}^6 \sum_{\pm} [\pm |F_{i,\pm}|^2]. \quad (22)$$

Note that the asymmetry Σ is defined here with a different sign as compared to that in Ref. [35] (cf. the recent review [36] and references therein).

In the following we present the QGSM predictions for the asymmetry Σ and the polarization transfer to the proton, $C_{z'}$, for photon energies $E_\gamma = (1.2 \div 6)$ GeV. In Fig. 4 the QGSM results of the asymmetry Σ (dashed lines) - calculated for linearly polarized photons - are shown as a function of the photon energy E_γ for different angles θ_p^{CM} . The QGSM predicts a slow decrease of $\Sigma(90^\circ)$ with the photon energy from 0.6 (at 1.5 GeV) to 0.2 (at 5 – 6 GeV). Also at the other angles, the asymmetry Σ is a decreasing function of E_γ , although slightly smaller in absolute magnitude. At 6 GeV it can even become negative at 70° and 110° .

It is worth noticing that the behavior of the asymmetry Σ in the QGSM is quite different from the one predicted by the Hadron-Helicity Conservation (HHC) model as discussed in Refs. [28,37]. Moreover, according to Brodsky and Hiller [15], one should get $\lambda_d = \lambda_p + \lambda_n$ within pQCD independently

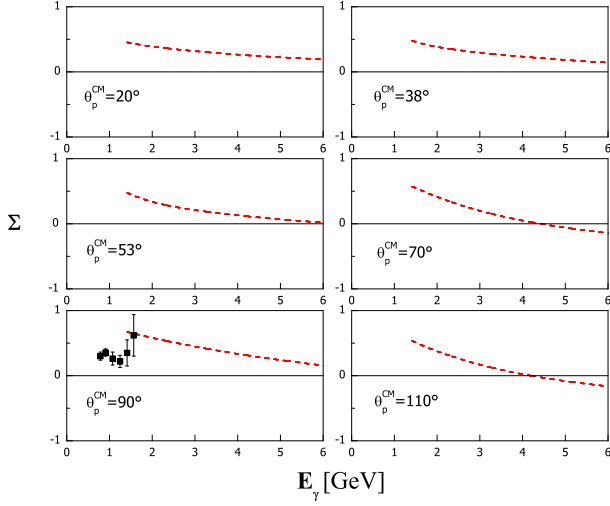


Fig. 4. The asymmetry Σ (23) for linearly polarized photons as a function of the photon energy for different θ_p^{CM} angles. The dashed lines are calculated within the QGSM for $R = 2$ while the experimental data are taken from Ref. [28]. The solid line for $\Sigma = 0$ is added to guide the eye.

of λ_γ . Assuming that - in the scaling limit - the transverse deuteron helicities are suppressed as compared to the longitudinal ones, the Σ asymmetry for linearly polarized photons

$$\Sigma(\theta) = (d\sigma_{||} - d\sigma_{\perp}) / (d\sigma_{||} + d\sigma_{\perp}) \quad (23)$$

at $\theta_p^{\text{CM}} = 90^\circ$ should approach the value [37]:

$$\Sigma(90^\circ) \simeq -2 \operatorname{Re}(F_{5,+} F_{5,-}^*) / (|F_{5,+}|^2 + |F_{5,-}|^2). \quad (24)$$

Using the axial symmetry $F_{5,+}(90^\circ) = F_{5,-}(90^\circ)$, Nagorny et al. [37] predicted that $\Sigma(90^\circ)$ should approach the value -1 . We note, however, that the condition $F_{5,+}(90^\circ) = F_{5,-}(90^\circ)$ is only valid for *isoscalar* photons, where the isospin function is antisymmetric. In the case of *isovector* photons, the isospin function is symmetric and, due to the Pauli principle, one has $F_{5,+}(90^\circ) = -F_{5,-}(90^\circ)$. Furthermore, according to the VMD model the isovector photon couples to hadrons more strongly than the isoscalar photon. Thus one expects that, in the case of hadron-helicity conservation, $\Sigma(90^\circ)$ should not be very different from $+1$ and, therefore, be significantly larger than the value predicted by the QGSM.

Also shown in Fig. 4 are the experimental data from Ref. [28] that are available only at $\theta_p^{\text{CM}} = 90^\circ$. The data are compatible with the QGSM predictions at 1.5 GeV: unfortunately at lower energies, where resonance amplitudes are important, the QGSM, as well as pQCD and related high-energy approaches, cannot be applied. Thus, polarization measurements at higher energies are necessary to discriminate between the models in a more adequate way.

In Fig. 5 the QGSM predictions of the polarization transfer $C_{z'}$ for circularly polarized photons are shown as a function of

E_γ at different θ_p^{CM} angles. It is interesting to note that the values of $C_{z'}$ from the QGSM are quite large and at $\theta_p^{\text{CM}} = 38^\circ$ almost reach the maximal value of ~ 1 above 2 GeV photon energy. This is directly related to the spin structure of the amplitude defined in Eq. (2).

Also shown in Fig. 5 are the experimental data available only at $\theta_p^{\text{CM}} = 90^\circ$ [4]; the latter have been corrected for spin rotation due to the lab-CM transformation. For photon energies $E_\gamma \geq 1.5$ GeV the data are in reasonable agreement with the QGSM results². Again, at lower energies resonant contributions to the amplitudes are expected such that a comparison should only be meaningful for photon energies above about 2 GeV.

The difference in the absolute value of $C_{z'}$ between the present values and those given in Ref. [38] is related to the effect of the forward-backward angle asymmetry of the amplitude, which was not taken into account there for polarization observables. As we have learned now, this effect is quite important not only for the angular distribution of the differential cross section (cf. Fig. 2) but also for polarization observables.

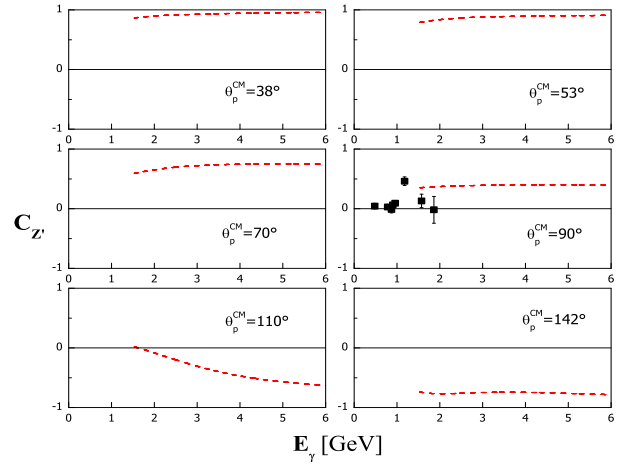


Fig. 5. Polarization transfer $C_{z'}$ for circularly polarized photons as a function of E_γ for different angles θ_p^{CM} . The dashed lines are calculated within the QGSM for $R = 2$ while the experimental data are taken from Ref. [4] and have been corrected for spin rotation due to the lab-CM. transformation. The solid line for $C_{z'} = 0$ is added to guide the eye.

We finally note, that the analysis of the asymmetries $C_{x'}$ and P_y is much more involved because it is sensitive to the relative phase of the helicity amplitudes (which might also depend on the final-state interaction of the np system). In this respect calculations of $C_{z'}$ and Σ are more stable because they do not depend on this phase, but only (for $C_{z'}$) or mainly (for Σ) on the moduli squared of the helicity amplitudes.

² In our previous calculations in Ref. [38] at $\theta_p^{\text{CM}} = 90^\circ$ there was an error in the sign of $C_{z'}$ which is corrected now.

6 Summary

The deuteron photodisintegration has been studied within the Quark-Gluon String Model, employing a logarithmic nucleon Regge trajectory (8). The angular distributions obtained have been compared to the data available, which nicely confirm the forward-backward angle asymmetry predicted by the model.

In addition, new results from the QGSM for the polarization transfer to the proton, $C_{z'}$ and the cross section asymmetry, Σ , for photon energies (1.2 ÷ 6) GeV and at different proton CM-angles, θ_p^{CM} , have been calculated. The results have been compared to the data available only at $\theta_p^{\text{CM}} = 90^\circ$ and up to 2 GeV; for photon energies ≥ 1.5 GeV the data are found in reasonable agreement with the QGSM results. Since contributions from resonant amplitudes should be present in the data, a meaningful comparison with the QGSM results can only be performed for higher energies. Data at high energy should come up in the near future from Jlab [39] and will allow to discriminate between the different approaches discussed in this work.

We are grateful to Ronald Gilman for useful comments and for sending us the experimental data on the polarization transfer $C_{z'}$ in Fig. 5 corrected for spin rotation due to the lab-CM transformation. The work has been supported by the Italian Istituto Nazionale di Fisica Nucleare (INFN), the Russian Fund for Basic Research (grant 02-02-16783) and by the Federal Program of the Russian Ministry of Industry, Science and Technology No. 40.052.1.1.1112.

References

1. C. Bochna et al., *Phys. Rev. Lett.* **81**, 4576 (1998).
2. E.C. Schulte et al., *Phys. Rev. Lett.* **87**, 102302 (2001).
3. S.J. Brodsky and G.R. Farrar, *Phys. Rev. Lett.* **31**, 1153 (1973); V. Matveev, R.M. Muradyan, A.N. Tavkhelidze, *Lett. Nuovo Cimento* **7**, 719 (1973).
4. K. Wijesooriya et al., *Phys. Rev. Lett.* **86**, 2975 (2001).
5. V.Yu. Grishina et al., *Eur.Phys.J. A* **10**, 355 (2001).
6. L.A. Kondratyuk et al., *Phys. Rev. C* **48**, 2491 (1993).
7. A.B. Kaidalov, *Z. Phys C* **12**, 63 (1982).
8. A.B. Kaidalov, *Surv. High Energy Phys.* **13**, 265 (1999).
9. D.D. Coon et al., *Phys. Rev. D* **18**, 1451 (1978).
10. M. Arik, *Phys. Rev. D* **19**, 3467 (1974).
11. Z. Chikovani, L.L. Jenkovszky, F. Paccanoni, *Mod. Phys. Lett. A* **6**, 1409 (1991).
12. H. Ito, *Prog. Theor. Phys.* **84**, 94 (1990).
13. A.I. Bugrij, G. Cohen-Tannoudji, L.L. Jenkovszky, and N.I. Kobylinsky, *Fortschr. Phys.* **31**, 427 (1973).
14. M.M. Brisudová, L. Burakovsky and T. Goldman, *Phys. Rev. D* **61**, 054013 (2000).
15. S.J. Brodsky and J.R. Hiller, *Phys. Rev. C* **28**, 475 (1983).
16. M. Guidal, J.M. Laget and M. Vanderhaeghen, *Nucl. Phys. A* **627**, 645 (1997).
17. R. Fiore et al., *Phys. Rev. D* **60**, 116003 (1999).
18. C. White et al., *Phys. Rev. D* **49**, 58 (1994).
19. M. Battaglieri et al., *Phys. Rev. Lett.* **87**, 172002 (2001).
20. R. Crawford et al., *Nucl. Phys. A* **603**, 303 (1996).
21. J. Napolitano et al., *Phys. Rev. Lett.* **61**, 2530 (1988).
22. S.J. Freedman et al., *Phys. Rev. C* **48**, 1864 (1993).
23. J.E. Beltz et al., *Phys. Rev. Lett.* **74**, 646 (1995).
24. E.C. Schulte et al., *Phys. Rev. C* **66**, 042201 (2002).
25. M. Mirazita et al., Proc. Int. Workshop Meson 2002, May 24-28, 2002, Cracow, Poland; eds. L. Jarczyk, M. Magiera, C. Guaraldo, H. Machner, World Scientific Publishing 2003, p. 413.
26. F. Ronchetti et al., Proc. Int. Conf. on Quarks and Nuclear Physics 2002 (QNP2002), June 9-14, Jülich, Germany; *Eur. Phys. J. A* (in print)
27. P. Rossi for the CLAS Collaboration, hep-ex/0302029.
28. F. Adamian et al., *Eur.Phys.J. A* **8**, 423 (2000).
29. A.C. Irving and R.P. Worden, *Phys. Rep.* **34**, 117 (1977).
30. A.B. Kaidalov, *Sov. J. Nucl. Phys.* **53**, 872 (1991).
31. C. Guaraldo, A.B. Kaidalov, L.A. Kondratyuk, Ye.S. Golubeva, *Yad. Fiz.* **59**, 1896 (1996); *Phys. Atom. Nucl.* **59**, 1395 (1996).
32. L.L. Frankfurt et al., *Phys. Rev. Lett.* **84**, 3045 (2000).
33. A.E.L. Dieperink and S.I. Nagorny, *Phys. Lett B* **456**, 9 (1999).
34. B. Julia-Diaz and T.-S.H. Lee, nucl-th/0210082.
35. V.P. Barannik et al., *Nucl. Phys. A* **451**, 751 (1998).
36. R. Gilman and F. Gross, *J.Phys. G* **28**, R37 (2002).
37. S.I. Nagornyi, Yu. A. Kasatkin, and I.K. Kirichenko, *Sov. J. Nucl. Phys.* **55**, 189 (1992).
38. V.Yu. Grishina et al., Proc. Int. Conf. on Quarks and Nuclear Physics 2002 (QNP2002), June 9-14, 2002, Jülich, Germany; *Eur. Phys. J. A* (in print); nucl-th/0209076.
39. R. Gilman, private communication.